TDAE chemisorbed on gold



2008 J. Phys.: Condens. Matter 20 315008

(http://iopscience.iop.org/0953-8984/20/31/315008)

J. Phys.: Condens. Matter **20** (2008) 315008 (9pp) doi:10.1088/0953-8984/20/31/315008

# TDAE chemisorbed on gold

**Johan Böhlin, Mikael Unge and Sven Stafström**

Department of Physics, Chemistry and Biology, IFM, Linköpings Universitet, SE-581 83 Linköping, Sweden

E-mail: joboh@ifm.liu.se, mikun@ifm.liu.se and sst@ifm.liu.se

Received 20 December 2007, in final form 18 May 2008
Published 8 July 2008
Online at stacks.iop.org/JPhysCM/20/315008

**Abstract**

DFT calculations on tetrakis(dimethylamino)ethylene (TDAE) interacting with a gold surface have been performed. A monolayer of TDAE deposited on a gold surface creates an interface dipole, which decreases the barrier for electron injection from a gold contact into an (organic) electroactive material. This was studied by simulating the complex in two different ways, using a slab model and using a gold cluster surface. These approaches are shown to be complementary: the cluster results apply to the situation of isolated molecules and the slab results describe the case of interacting TDAE molecules on the gold surface. We found that there is a transfer of around one electronic charge per TDAE to the gold in the limit of non-interacting TDAE molecules. This charge transfer results in the formation of an interface dipole and a corresponding lowering of the work function of the surface. The lowering of the work function increases with increasing coverage and is as large as 2.4 eV for a monolayer of TDAE on gold. Due to depolarization effects, the charge transfer in this state is reduced to 0.56 times the electronic charge.

(Some figures in this article are in colour only in the electronic version)

## 1. Introduction

The barrier for charge injection in electronic devices can be controlled by a molecular layer between the contact and the semiconducting material. This has been demonstrated for organic semiconductors (Campbell *et al* 1996, 1997) as well as for GaAs (Vilan *et al* 2000), Si (Salzer and Cahen 2001) and ZnO (Salomon *et al* 2003). The change in the injection barrier occurs as a result of the creation of a dipole at the interface, which in turn affects the work function of the contact. Depending on magnitude and direction of the dipole the work function of the contact could be either decreased or increased (Campbell *et al* 1996).

The interface dipole can have three major components (Crispin *et al* 2002). One component originates from the shortening of the surface electron density tail upon molecular adsorption (Bagus *et al* 2002, Lang 1971). This is a purely quantum mechanical phenomenon, which arises from exchange (or Pauli) repulsion (Bagus *et al* 2002). A second component comes from the intrinsic dipole of the adsorbed molecule that is normal to the surface. The third component is the chemical dipole which results from rearrangement of charge as a result of chemisorption of the molecule on the surface. Although all three components can have substantial effects on the work function (Crispin *et al* 2002), the most recent studies have been focused on the importance of the chemical dipole. One type of chemical dipole results from covalent bonding at metal–molecule interfaces. The charge rearrangement occurs in this case at the local scale which results in a series of dipole layers at the interface (Heimel *et al* 2006, Rusu and Brocks 2006). Another type of dipole layer occurs as a result of charge transfer from the molecule to the contact surface. One example of a molecule which has this behavior is tetrakis(dimethylamino)ethylene (TDAE) (see figure 1). TDAE is very electron rich and has a first ionization potential comparable to that of alkaline metals (Bock *et al* 1991). The electron transfer is thus from the molecule to the contact surface and the dipole is pointing in the direction of the surface normal and results in a lowering of the vacuum level electrostatic potential and a corresponding lowering of the work function of the surface. A monolayer of TDAE on indium tin oxide leads to a decrease of the work function by 0.9 eV (Osikowicz *et al* 2004), and in a very recent experimental study of TDAE deposited on a gold surface it was shown that the work function decreases by 1.3 eV (Lindell *et al* 2008).

The aim of this work is to get a detailed and quantitative understanding of the interaction between TDAE and a gold surface, in particular the extent of charge

 

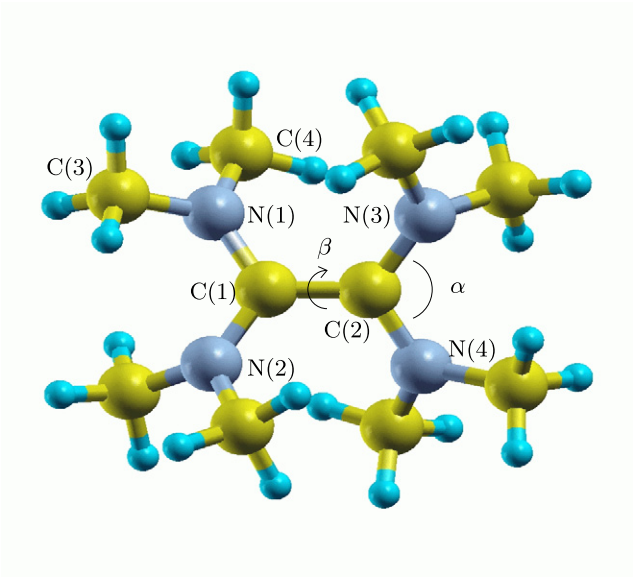


**Figure 1.** Schematic structure of TDAE.

transfer and the strength of the chemical dipole, the chemisorption energy, and the work function shift. Density functional theory (DFT) methods within the local density approximation (LDA) or generalized gradient approximation (GGA) have been successful in studies of chemisorbed species, because of the effective treatment of short-range electron correlation. Numerous studies using this methodology have been performed to describe molecular chemisorption (Lewis and Rappe 1999).

The calculations of the work function were performed using a crystal approach with a slab describing the interface and with a basis set consisting of plane waves. For comparative reasons we have also used a cluster approach for the same studies. The methodologies in both these approaches are described in section 2 below, followed by a presentation of the details of the chemical and physical properties of the TDAE/gold interface in section 3. Finally, in section 4 we summarize the results and discuss the implications of the observed work function shift on device applications.

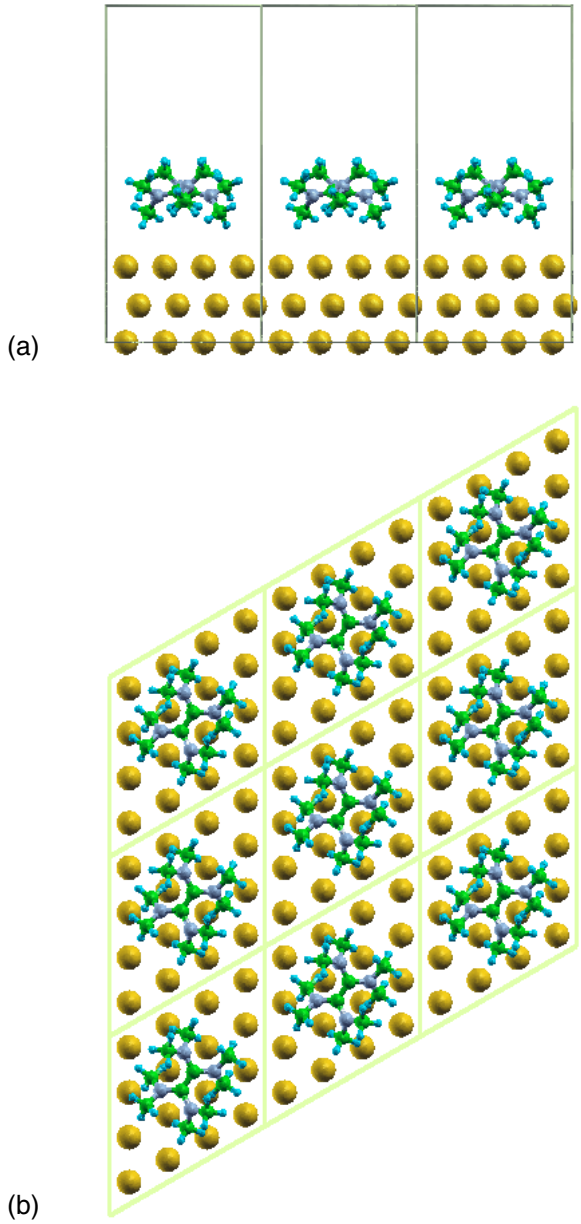


**Figure 2.** Side (a) and top (b) view of TDAE on Au(111). The c(4 × 4) surface unit cell is indicated by the contour in (a) and (b).

## 2. Methodology

Slab calculations were performed with the Vienna *ab initio* simulation package (VASP) (Kresse and Hafner 1993, Kresse and Furthmüller 1996a, 1996b), employing the Perdew–Burke–Erzerhofer (PBE) (Perdew *et al* 1996) exchange–correlation functional. A plane wave basis set with a kinetic energy cut-off of 400 eV was used. The gold surface was modeled using a periodically repeated slab (figure 2) with the two slab surfaces corresponding to the (111) cut of the gold crystal. Different coverages were modeled by different numbers of gold atoms per layer in the slab. For each such system, the adsorption of molecules is on one of the two slab surfaces. The slabs are separated by a vacuum region which is large enough to ensure no overlap of the wavefunctions between neighboring unit cells in the direction perpendicular to the gold surface. To avoid interaction between the periodical images of the slab the electrostatic potential is adjusted accordingly (Neugebauer and Scheffler 1992). The number of layers in the slab was set to three since test calculations showed that the physical properties related to chemisorption of TDAE converged for this slab thickness. The geometry of the TDAE molecule and the uppermost layer of the substrate was allowed to relax according to Hellmann–Feynman forces until the remaining forces were $<0.01$ eV Å$^{-1}$. All degrees of freedom were allowed to relax for the TDAE molecule. The second and third layer gold atoms had fixed positions using the lattice constant of 4.08 Å for the bulk crystalline material. The distance between layers was 2.355 Å. The Brillouin zone integration was performed using a $5 \times 5 \times 1$ Monkhorst–Pack grid, since test calculation showed that the physical properties

**Table 1.** Geometry parameters of TDAE from DFT calculations with different basis sets.

| | DFT | | | | | |
|---|---|---|---|---|---|---|
| | 6-31G | 6-31G* | cc-pVDZ | cc-pVTZ | Exp.[a] | |
| C(1)–C(2) | 1.372 | 1.370 | 1.372 | 1.364 | 1.36 | (Å) |
| C(1)–N(1) | 1.420 | 1.415 | 1.416 | 1.410 | 1.403 | (Å) |
| N(1)–C(3)[b] | 1.461 | 1.453 | 1.452 | 1.450 | 1.452 | (Å) |
| N(1)–C(4)[b] | 1.456 | 1.446 | 1.446 | 1.443 | 1.452 | (Å) |
| $\alpha$ | 113.6 | 112.5 | 112.5 | 112.8 | 118.4 | |
| $\beta$ | 30.3 | 32.1 | 31.4 | 31.1 | 28.2 | |

[a] From Bock *et al* (1991).

[b] Only one experimental value for these two distances is reported.

related to the chemisorption of TDAE converged for a grid this size. The width of the vacuum region above the topmost atom of the TDAE molecule was 10 Å.

From the result of the calculations of the slab we can determine the stability and the amount of charge transfer by comparing the chemisorption energy for different sizes of the unit cell and for different distances between the TDAE molecule and the gold surface in combination with population analysis using the Bader analysis (Henkelman *et al* 2006, Sanville *et al* 2007). The Bader analysis is based on so called zero-flux surfaces that are used to divide the three-dimensional space into sub-volumes occupied by one atom each. A zero-flux surface is the surface on which the charge density has a minimum. Typically in molecular systems this minimum occurs between atoms and introduces a natural way to separate atoms from each other.

In the cluster approach we performed first principles calculations of isolated TDAE molecules in different charged states as well as on TDAE interacting with gold clusters in the range from 20 to 46 gold atoms. The gold atoms were fixed to the positions of an ideal gold crystal. More details of the geometry of the gold clusters are presented together with the results below.

The calculations were carried out using the *Gaussian 03* program (Frisch *et al* 2004), with the B3LYP functional (Becke 1993, Lee *et al* 1988). Geometry optimizations of the different charged states of the isolated TDAE were performed with the 6-31G, 6-31G*, cc-pVDZ and cc-pVTZ basis sets. For the singly charged molecule the unrestricted method has been used. In the calculation of TDAE on gold, we used, for the light elements (H, C, N), the 6-31G basis set for the geometry optimization followed by calculations of charge densities, dipole moments, and chemisorption energies using the cc-pVDZ basis sets. The relativistic correct basis set LanL2DZ with the 19-electron effective core potentials was used for gold (Hay and Wadt 1985). Also in this case the TDAE molecule is absorbed on the (111) gold surface. The calculations using various gold cluster sizes are intended for analysis of the evolution of different properties with increasing cluster size. A single TDAE molecule is included for all cluster sizes. Thus, this approach does not include effects of intermolecular interactions.

From the result of the calculations of the complex we can determine the stability and the amount of charge transfer by comparing the chemisorption energy for different geometries of the molecule in combination with population analysis using Mulliken charges and natural population analysis (NPA) (Reed *et al* 1985) of the gold cluster and the molecule, respectively. (Unless otherwise specified Mulliken charges are used below.)

## 3. Results

### *3.1. TDAE*

The geometrical structure of the isolated TDAE molecule without any constraints concerning symmetry was first optimized using the *Gaussian 03* program (Frisch *et al* 2004). The resulting geometry has $D_2$ symmetry; see figure 1. The results are compared with experimental data in table 1.

The overall agreement is very good. In particular, we find better agreement for the dihedral angle, $\beta$, between the two N–C–N planes than in previously reported theoretical results (Tanaka *et al* 1996, Pederson and Laouini 1999, Fleurat-Lessard and Volatron 1998). This improvement can be explained by the fact that we use a non-local functional. Only small differences in bond lengths and angles are observed between a smaller (6-31G) and a larger basis set (cc-pVTZ). The energy minimum found by Fleurat-Lessard and Volatron (1998) was obtained by using a starting geometry from optimized tetrakis(amino)ethylene. This minimum is reproduced at the Hartree–Fock/6-31G* level. However, at the B3LYP/6-31G* level this structure does not correspond to an energy minimum; there is a small energy difference of 0.03 eV in favor of the geometry presented above. The geometry presented in table 1 is in much better agreement with experimental values than the geometry obtained by Fleurat-Lessard and Volatron (1998). Note, however, that since the experimental data show no indication of two nearly degenerate ground state geometries the calculated energy separation between the two structures is probably underestimated.

The changes in the molecular geometry upon oxidation were also calculated. The results are shown in table 2 for the TDAE cation. The calculated values follow the trend of the experimental values (Pokhodnia *et al* 1999). The C(1)–C(2) bond length increases and the C(1)–N(1) bond length decreases. These changes occur as a result of the nature of the highest occupied molecular orbital, which is bonding in the C(1)–C(2) bond and anti-bonding in the C(1)–N(1) bond. By removing electrons from this orbital the bond order changes, which in turn affects the bond distances and torsion angles according to the results shown in table 2.

**Table 2.** Geometry parameters of TDAE, $TDAE^+$ and the TDAE/gold complex. The cc-pVDZ basis set was used in the calculations of the molecule and in the cluster calculation.

| | TDAE | | $TDAE^+$ | | Complex | | | |
|---|---|---|---|---|---|---|---|---|
| | DFT | Exp.[a] | DFT | Exp.[b] | Cluster | Slab 4 × 4 | Slab 6 × 6 | |
| C(1)–C(2) | 1.372 | 1.36 | 1.431 | 1.415 | 1.411 | 1.416 | 1.422 | (Å) |
| C(1)–N(1) | 1.416 | 1.403 | 1.374 | 1.367 | 1.392 | 1.385 | 1.382 | (Å) |
| N(1)–C(3)[c] | 1.452 | 1.452 | 1.461 | 1.456 | 1.465 | 1.453 | 1.454 | (Å) |
| N(1)–C(4)[c] | 1.446 | 1.452 | 1.459 | 1.456 | 1.464 | 1.452 | 1.453 | (Å) |
| $\alpha$ | 112.5 | 118.4 | 118.3 | 119 | 116.70 | 116.55 | 116.799 | |
| $\beta$ | 31.4 | 28.2 | 36.8 | 42 | 28.77 | 28.82 | 28.632 | |

[a] From Bock *et al* (1991).
[b] From Pokhodnia *et al* (1999).
[c] Only one experimental value for these two distances is reported.

### *3.2. TDAE–gold cluster*

Before we turn to the calculations of the work function we discuss the basic features of chemisorption of TDAE on gold. Some of these features, in particular those that relate to the properties of the TDAE molecule, can be better described in the cluster model. Therefore we begin the presentation by discussing the results of this approach.

The gold (111) surface was modeled in the calculations by clusters with four different sizes: 20, 26, 32, and 46 atoms. The clusters have three layers, a top (second (Sellers *et al* 1993)) layer with 13 (6), 13 (12), 19 (12), and 25 (21) atoms in the $Au_{20}$, $Au_{26}$, $Au_{32}$, and $Au_{46}$ clusters, respectively. A third layer, a single atom, is introduced in the $Au_{20}$, $Au_{26}$, and $Au_{32}$ clusters to get an even number of gold atoms and a closed shell system. All Au–Au bond distances are set to 2.88 Å.

TDAE is positioned in such a way that the axis through the C(1)–C(2) bond is parallel to the surface and the midpoint of the C(1)–C(2) bond is above the center gold atom in the cluster. We introduce a variable $r$ for this distance. Since the TDAE molecule interacts with several of the gold atoms with mostly non-directional bonds (see below), the chemisorption energy is less sensitive to the exact position of the molecule (Crispin *et al* 2002). We therefore fix the position of the midpoint of the C(1)–C(2) bond to that above the center gold atom in all cluster calculations. (As will be discussed below, this restriction can be avoided in the slab calculation.)

The distance $r$ was varied in a set of calculations of the chemisorption energies of the TDAE/$Au_{20}$ complex. The chemisorption energy, $\Delta E$, is defined as

$$\Delta E = (E_{\text{Tot.}}^{\text{Complex}} - (E_{\text{Tot.}}^{\text{TDAE}} + E_{\text{Tot.}}^{\text{Au}_n})). \qquad (1)$$

We let the internal structure of the molecule relax on the surface. A minimum in the chemisorption energy was obtained for $r = 5.0$ Å. The chemisorption energy is 0.73 eV. At the energy minimum, the C(1)–C(2) bond is 1.41 Å and the N(1)–C(1) bond distances are approximately 1.39 Å. These values lie between the bond distances of the neutral and singly charged TDAE, which indicates that the effective charge transfer is less than one electron. The dihedral angle is 28°, which is considerably smaller than in the singly charged molecule in the gas phase and also smaller than in the neutral molecule. The shortest (average) hydrogen gold surface distance is 2.8 Å (4.91 Å).

**Table 3.** Net charge on the TDAE molecule, $\Delta q$, in units of elementary charge, using Mulliken population analysis and natural population analysis (NPA) and the induced dipole moment, $\Delta\mu$, in Debye. All results are obtained using the cc-pVDZ basis set.

| | Mulliken | NPA | $\Delta\mu$ |
|---|---|---|---|
| TDAE/$Au_{20}$ | 0.90 | 0.68 | 12.6 |
| TDAE/$Au_{26}$ | 1.07 | 0.84 | 17.5 |
| TDAE/$Au_{32}$ | 1.16 | 0.87 | 16.4 |
| TDAE/$Au_{46}$ | 1.23 | 0.81 | 16.8 |

In order to study the effect of the cluster size we increased the cluster size to $Au_{26}$, $Au_{32}$, and $Au_{46}$ in the way described above. The charge transfer from TDAE to gold for the different complexes is shown in table 3 in the cc-pVDZ basis set. Values from both Mulliken and natural population analysis (NPA) (Reed *et al* 1985) are shown. The Mulliken charges are increasing for increasing cluster size whereas the NPA charges reach a maximum for the $Au_{32}$ cluster and then reduce slightly for the considerably larger $Au_{46}$ cluster. It is not the aim of this work to present a detailed quantitative analysis of these values. It is well known that there are drawbacks to using the Mulliken and NPA charge concepts. We can conclude, however, that in combination with the geometrical data presented above we have presented results that indicate a net charge on the TDAE molecule of close to a unit positive charge.

The transfer of electronic charge from TDAE to the gold cluster results in an induced dipole moment, $\Delta\mu$. These induced dipole moments are calculated from the difference in the dipole moments in the direction perpendicular to the (111) surface of the gold cluster ($z$-direction) between the pristine gold cluster and the cluster/TDAE complex. $\Delta\mu$ is of particular interest in the context of work function shifts, which will be discussed in more detail below in connection with the results of the slab calculation. In these discussions we will also include the results of the cluster calculations, which are presented in table 3. We note from these results that there is an overall qualitative agreement between $\Delta q$ values and $\Delta\mu$ as a function of increasing cluster size. The induced dipole moments appear to converge to a value of about 16–17 D. This value can be compared with the dipole moment of an

ideal point charge electric dipole with a separation distance of $r = 5.0$ Å, which is 24 D for unit charges. This discrepancy can be explained by the combination of two factors, a net charge transfer which is less than unity (as indicated by the results of the NPA), and an effective separation distance which is less than 5 Å (see discussion below).

The chemisorption energies for the $Au_{26}$, $Au_{32}$ and $Au_{46}$ complexes using the cc-pVTZ basis set are 0.90 eV, 1.01 eV and 0.83 eV, respectively. These variations can partly be explained by the different amount of charge transfer in the three complexes and are in better agreement with the NPA charges. We have also studied the effect of small changes in the cluster shape by using different positions of the ideal Au crystal for the individual atoms. Such rearrangements only cause minor differences compared to the difference in chemisorption energies and charge transfer between the clusters of different size. On the basis of these observations we can conclude that the decrease in the amount of (NPA) charge transfer in the TDAE/$Au_{46}$ complex compared to the TDAE/$Au_{32}$ complex is not related to details of the shape of the cluster. For clusters smaller than and including $Au_{32}$ there are edge states that form weak covalent bonds to the methyl groups closest to the gold surface. For the corresponding state in the TDAE/$Au_{46}$ complex all interactions are with gold atoms in the interior of the surface. The fact that edge atoms, that are more reactive, do not contribute to the bonding for this cluster explains the decrease in charge transfer and chemisorption energy for the largest cluster compared to TDAE/$Au_{32}$ complex.

We conclude from our studies of TDAE chemisorbed on the (111) surface of a gold cluster that individual geometrical parameters are fairly independent of the size of the gold cluster, whereas quantities that are related to the complex as a whole, e.g. $\Delta q$, $\Delta\mu$ and $\Delta E$, show small and non-systematic variations with increasing cluster size. In the next section we will compare these quantities with the corresponding quantities calculated using the slab geometry.

### *3.3. Slab calculation*

The gold (111) surface was modeled in the calculations by slabs with three layers and with six different unit cells with layer sizes: $3 \times 4$ atoms, $4 \times 4$ atoms, $5 \times 4$ atoms, $5 \times 5$ atoms, $6 \times 5$ atoms and $6 \times 6$ atoms. The top layer was allowed to relax both in the calculation of the isolated slab system and in the presence of TDAE. This relaxation results in both cases in a motion of the gold atoms in the top layer towards the second gold layer by ∼0.15 Å. The additional relaxations of the gold atoms in the presence of the TDAE molecule are very small, less than 0.02 Å.

In table 2 are shown the optimized bond lengths, bond angles and central torsion angle of TDAE on the gold (111) surface for the layer sizes of $4 \times 4$ and $6 \times 6$ gold atoms, which correspond to a nearly ideal monolayer coverage (see below) and the lowest coverage that we have considered, respectively. In comparison with the results of the cluster model we find that the two different approaches give rather similar results. In the case of $4 \times 4$ gold atoms the TDAE molecules are interacting and, as a result of depolarization (see below) less charged.

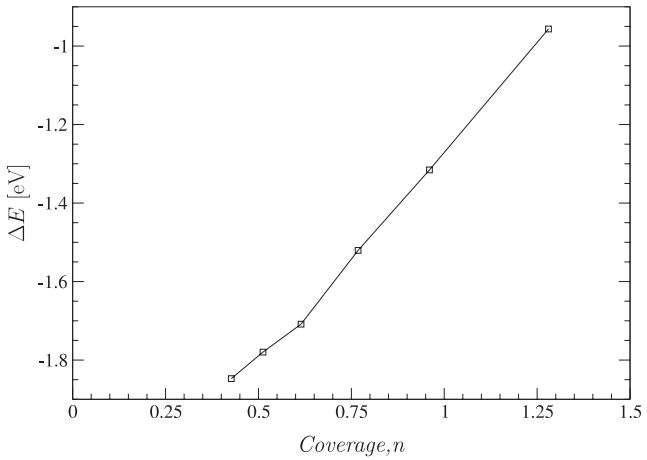


**Figure 3.** Chemisorption energy per unit cell as a function of TDAE coverage. The coverage $n$ is defined as $n = A/A_0$, where $A$ is the unit cell area and $A_0$ is the area of the TDAE molecule, estimated as $7.7 \times 8.3$ Å$^2$ (see text).

This has a small but notable effect on the geometry. For the larger unit cell of $6 \times 6$ atoms, the C(1)–C(2) bond length is slightly elongated whereas all other bond lengths and bond angles remain essentially unchanged as compared to the case of monolayer coverage. The elongated C(1)–C(2) bond is fully consistent with the additional charging of the TDAE molecule, as can be seen from the change in this bond length going from the neutral to the charged state.

As concerns the position of TDAE on gold, we can perform a full relaxation of the molecule in the slab model. This was impossible in the cluster approach since the cluster boundaries act as spurious chemisorption sites. The molecule is found to lie flat on the slab surface and the intermolecular orientation is that presented in figure 2. The optimized distance between the gold surface and the center of the molecule is $r = 5.0$ Å. The reference position on the gold system is in this case the position of the unrelaxed surface. This reference is used in order to allow for a direct comparison with the cluster results in which the gold surface is fixed. We have used this reference for the results presented in both figures 3 and 7 below. The additional relaxation of the topmost gold layer by ∼0.15 Å should be added in order to get the actual separation distance.

The chemisorption energies obtained from the slab calculations are shown in figure 3 as a function of the molecular coverage of the surface. The coverage $n$ is defined as $n = A/A_0$, where $A$ is the unit cell area and $A_0$ is the area of the TDAE molecule. The area of a single molecule is obtained from the van der Waals radii of the constituent atoms and is estimated to be $7.7 \times 8.3$ Å$^2$. The $4 \times 4$ system represents near unit coverage (0.96 to be precise), which hereafter is referred to as monolayer coverage. This system is used below as a model system of the TDAE/gold interface.

For the largest system shown in figure 3, $E = -1.85$ eV (coverage 0.43 or $6 \times 6$ gold atoms per slab layer). This energy is approximately 1 eV larger than the value obtained for the cluster system ($-0.85$ eV). To some extent, this difference is due to the fact that we allow the gold surface to relax (both with and without TDAE present) in the slab calculation but not

in the cluster approach. Using the same geometry for the gold atoms as in the cluster calculation the chemisorption energy reduces to −1.65 eV (coverage 0.43). This is still considerably larger than the value obtained in the cluster approach, which shows that most of the difference can be ascribed to finite size effects of the cluster. The additional electronic charge is forced to distribute over a smaller gold surface area when restricted to the cluster. This results in higher charge densities and stronger internal Coulomb repulsion. In the slab system, the charge distribution is not subject to such boundary effects. The results from the slab calculations therefore give a more accurate estimate of the chemisorption energy of TDAE on gold.

With increasing coverage the molecules come closer to each other and the intermolecular interactions start to contribute to the chemisorption energy. In reality, these interactions include the repulsive electrostatic interactions between the dipoles of each unit cell and the attractive dispersive (van der Waals) intermolecular interactions. Since none of the currently used functionals in DFT correctly account for electron–electron correlations between two separate charge densities (Kristyan and Pulay 1994, Silva *et al* 2003), the van der Waals interactions are incomplete in our treatment. However, since the electrostatic interactions are much larger than the van der Waals forces for the dipole strengths considered here, the chemisorption energies calculated from the slab model are representative for the TDAE/gold interface.

The chemisorption energy decreases with decreasing layer size, from 1.85 eV for the $6 \times 6$ system down to 1.32 eV for the $4 \times 4$ system, which corresponds to full monolayer coverage of the surface. For even more densely packed molecules there is a sharp decrease to 0.96 eV for the $3 \times 4$ system (coverage 1.28). This reduction in chemisorption energy is directly related to the electrostatic interactions that result from the net charges residing on the surface and the TDAE molecule. We will discuss this issue in more detail in relation to the results of the work function shift also shown in figure 6 below. However, before we begin this discussion it is useful to have more information concerning the charge transfer and the change in electrostatic potential that occur as a result of TDAE adsorbed on the surface.

The charge reorganization upon deposition is given by the difference between the superimposed charge densities of the isolated slab and the isolated molecule and the equilibrated density of the gold(111)-TDAE complex. We present these results in terms of the plane-integrated charge density $\Delta\rho(z)$ in units of elementary charge $e$ Å$^{-1}$ according to

$$\Delta\rho(z) = \int\int_{\text{unit cell}} [\rho_{\text{Complex}} - (\rho_{\text{molecule}} + \rho_{\text{slab}})]\,\mathrm{d}x\,\mathrm{d}y. \tag{2}$$

In figure 4 is shown both $\Delta\rho(z)$ and the integrated charge difference, $\Delta q(z)$ (this quantity is also given in units of the elementary charge), from the bottom of the gold slab ($z = 0$) to well above the TDAE molecule ($z = 14$ Å) of the $4 \times 4$ system. The deviations from $\Delta\rho(z) = 0$ are observed near the gold surface towards the molecule. Large positive values, i.e. an excess of electrons, occur between $z = 5$ and 6 Å, i.e., just

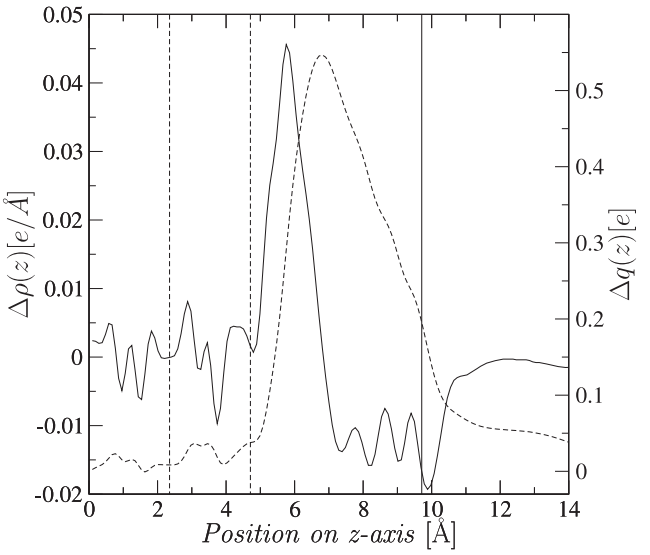


**Figure 4.** Plane-integrated charge density $\Delta\rho(z)$ in units of $e$ Å$^{-1}$ (solid line, left vertical axis) and the integrated charge difference $\Delta q(z)$ in units of $e$ (dashed line, right vertical axis). The vertical dashed lines show the positions of the gold atoms, the solid line the center of the molecule.

outside the gold surface. The negative values are fairly evenly distributed over the region of the molecule (7 Å $< z <$ 11 Å).

The integrated charge density provides a measure of the charge transfer. It reaches a maximum value of $\Delta q(z = 7\text{ Å}) = 0.56$ near the position of the TDAE atoms closest to the gold surface. This graphical way to determine the charge transfer is similar to performing the Bader analysis, which also gives the value of 0.56 for the charge transfer. This value is considerably smaller than the value of 0.81 obtained from the NPA of the largest cluster complex. Note, however, that in the latter case the charge associated with the molecule is related to the basis set used (see above) and as such has a non-local behavior. In the crystal calculations, for which a three-dimensional grid is used to describe the spatial variations in the charge density, the separation between the molecule and the gold surface is entirely geometrical (local). A direct comparison between these two quantities is therefore not justified. However, as will be discussed below, using indirect measures such as the induced dipole moment it is clear that the charge transfer in the $4 \times 4$ system is smaller than in the case of the cluster. The main reason for this difference is the depolarizing effect of the electric field of the surrounding unit cells.

We consider now the work function of the TDAE modified gold surface. The top panel in figure 5 shows the plane-averaged electrostatic potentials, $V_{\text{ES}}$ along the (111) direction ($z$-axis) with and without TDAE present on the gold surface. As discussed above, the electrostatic potential has to be adjusted in order to match the potential of the neighboring slab unit cell (Neugebauer and Scheffler 1992). This adjustment is, however, occurring at $z$-values outside the region shown in figure 5.

The dashed curve shows the potential of a clean gold surface and the solid curve the potential for the $4 \times 4$ surface

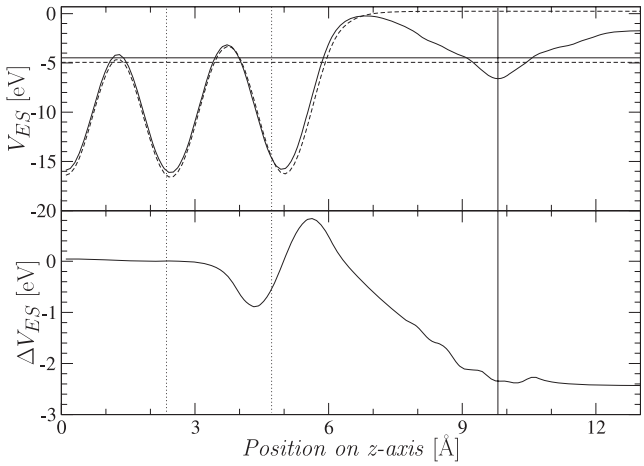


**Figure 5.** Top panel: plane-averaged electrostatic potential, $V_{\mathrm{ES}}$, for a clean gold surface (dashed line) and for the $4 \times 4$ surface with a chemisorbed TDAE molecule (solid line). The two horizontal lines show the corresponding Fermi energies. Bottom panel: the difference in plane-averaged electrostatic potential, $\Delta V_{\mathrm{ES}}$, between the sum of the potentials of the clean gold surface and the isolated TDAE molecule, and the potential with TDAE present on the gold surface. The position of the TDAE molecule is indicated by the solid vertical line, which coincides with the central C–C bond (atoms C(1) and C(2) in figure 1) of the molecule. In the case of the isolated TDAE molecule the potential has been shifted to this position. The dotted vertical lines show the positions of the two topmost gold layers.

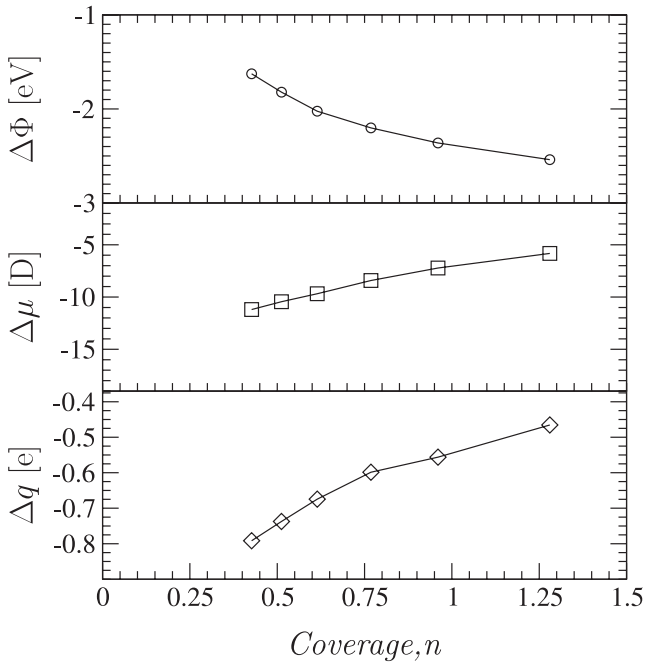


**Figure 6.** Work function shift (top panel), induced dipole moment, $\Delta\mu$ (middle panel), and charge transfer between molecule and surface (lower panel), as a function of the coverage, $n$, defined as the relation between the area of the TDAE molecule and the unit cell area.

with a chemisorbed TDAE molecule. The two horizontal lines show the corresponding Fermi levels.

Naturally, in the region around the molecule, the potential is strongly affected since the additional charge of the molecule cannot be screened as effectively as near to the metallic surface. Most interestingly, we notice a substantial change in $V_{\mathrm{ES}}$ in the vacuum regime away from the interface region. Since the work function, $\Phi$, is the difference in energy between the electrostatic potential in the vacuum region and the Fermi energy (Campbell *et al* 1996, DeRenzi 2005, Heimel *et al* 2006), this change in the electrostatic potential contributes to a lowering of the work function of the gold surface. Furthermore, the shift in the Fermi energy of the complex, which occurs as a result of electron transfer to the gold surface, gives another contribution to the lowering of the work function of the complex.

The spatial location of the changes in the potential become more evident from the lower panel of figure 5, which shows the difference in the electrostatic potential, $\Delta V_{\mathrm{ES}}$, between the sum of the potentials of the clean gold surface and the isolated TDAE molecule, and the potential with TDAE present on the gold surface. The large differences naturally occur at the gold surface and in the region of the molecule. Near the surface there is a shift in the potential curve such that the $V_{\mathrm{ES}}$ decreases upon TDAE deposition just below the gold surface and increases just above the surface. This is an effect of Pauli repulsion, which pushes the tail of the electron distribution towards the gold surface. The net effect is that the intrinsic surface dipole moment is slightly reduced in strength, with a corresponding net reduction in the electrostatic potential in the region 5 Å $< z <$ 6 Å. This effect is, however, closely

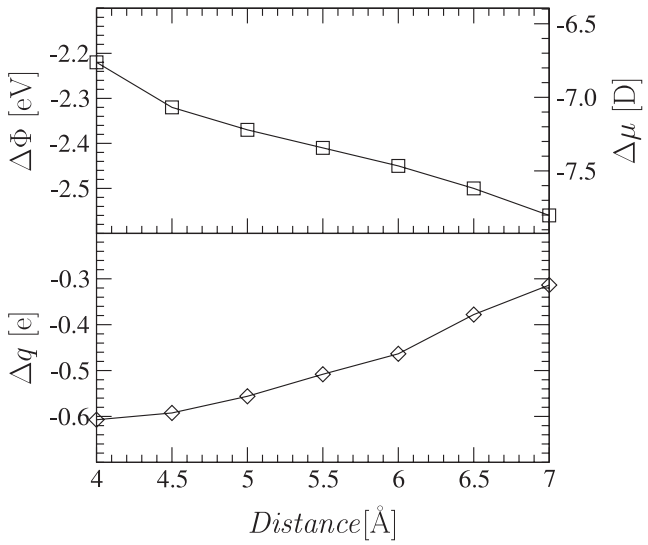


**Figure 7.** Work function shift (top panel) and the charge transfer (lower panel) between molecule and surface as a function of the distance between the center of the molecule and the gold surface.

associated with the lowering of the electrostatic potential due to the chemical dipole which dominates (see below) the change in the work function.

The difference in energy between the work function for the clean gold surface and the TDAE/gold complex defines the work function shift, $\Delta\Phi$, according to

$$\Delta\Phi = \Phi_{\mathrm{Complex}} - \Phi_{\mathrm{Au}}. \tag{3}$$

Figure 6 (top panel) shows the change in work function, $\Delta\Phi$ as a function of coverage of the surface. The change is calculated as the difference in work function between the surface and the complex; see equation (3). Even at low coverage, e.g. 0.43, the work function shift is as large as 1.63 eV. For increasing coverage the shift increases, and at unit coverage it is 2.36 eV. The experimentally reported shift of 1.3 eV (Lindell *et al* 2008) indicates that the TDAE coverage is far from complete in the measured sample. However, without any information about the coverage it is difficult to make a direct comparison between theory and experiment in this case.

The dependences on coverage of both $\Delta\Phi$ and $\Delta E$ are naturally strongly correlated and occur as a result of the increase in electrostatic interaction between the charges associated with the TDAE/gold complex. The change in work function is also directly related to the induced dipole moment, $\Delta\mu$, according to

$$\Delta\Phi = \frac{e}{\varepsilon_0}\frac{\Delta\mu}{A} = \frac{e}{\varepsilon_0 A_0}\Delta\mu n, \tag{4}$$

where $A$ ($A_0$) and the coverage $n = A_0/A$ were introduced above. The induced dipole moments are shown in the middle panel in figure 6 as a function of $n$. The decreasing (absolute) value of $\Delta\mu$ with increasing coverage is consistent with the sub-linear increase in the change in the work function with increasing coverage (see figure 6). This behavior of $\Delta\mu$ shows, in turn, that the charge transfer reduces with increasing coverage, which also explains the reduction in chemisorption energy with increasing coverage. Using the Bader analysis we obtain explicit values for the amount of charge transfer (lower panel, figure 6). In the range of coverage included in our calculation the results go from $\Delta q = 0.79$ at $n = 0.43$ to $\Delta q = 0.47$ at $n = 1.28$. It is important to note that in the regime of monolayer coverage, which is the most interesting regime from an application point of view, the charge transfer is far from that obtained in the cluster calculation, which completely neglects the effects of depolarization. The cluster result, on the other hand, is better suited to describe the regime of non-interacting dipoles, since even for the largest unit cells that can be treated in the slab calculations the depolarization effects are considerable. A detailed analysis of the transition between these two regimes lies outside the scope of this work.

In the near future we hope to be able to extend our calculations to even larger unit cells and to compare our results, based on quantum mechanical calculations, with the results of the widely used classical Topping model (Topping 1927, Lüth 1995).

In order to understand the influence of the different contributions to the total dipole, we have also studied how the work function shift depends on the separation distance $r$. If the surface dipole due to Pauli repulsion, which indeed can cause significant work function shifts (Witte *et al* 2005), were the dominant effect, the shift in the work function should decrease with increasing $r$. We have performed calculations for a set of $r$-values around the equilibrium position. In figure 7 are shown the values of $\Delta\Phi$ and $\Delta q$ (obtained from the Bader analysis). The calculation is performed for the $4 \times 4$ surface, for which the equilibrium position occurs at 5.0 Å above the (unrelaxed) gold layer. Clearly, the trend is opposite to that caused by Pauli repulsion, which is clear evidence that the chemical dipole dominates the work function shift. However, it is notable that the increase in the work function shift with increasing distance is not proportional to the increase in $r$. The explanation for this is given by the change in the charge transfer, which reduces with increasing distance, in this case from $\Delta q = 0.56$ at the equilibrium separation down to $\Delta q = 0.31$ at $r = 7.0$ Å. Note also that the change in the dipole follows exactly the work function shifts, since these two quantities only differ by a constant in the case of constant coverage (see equation (4)).

## 4. Summary and conclusions

The results presented above show that TDAE binds to a gold (111) surface with a strong chemical bond. The chemisorption is to a large extent due to electron transfer from TDAE to gold. In our theoretical studies based on density functional theory we have used both a cluster and a slab to model the gold surface. The optimized geometrical structure of the chemisorbed TDAE molecule is nearly identical in these two cases. The amount of charge transfer is not uniquely defined but it can be obtained indirectly by comparing the ground state geometry of TDAE on gold with the optimized geometries of TDAE with different ionicities. From such a comparison it is clear that the effective electron transfer is less than one electron. The equilibrium distance from the central part of the molecule to the gold surface is around 5.0 Å. This rather large charge separation distance results in a considerable electrostatic dipole moment for each molecule chemisorbed on the surface. The contribution of these dipoles to the electrostatic potential $V_{\mathrm{ES}}$ results in a lowering of the vacuum level potential and a corresponding lowering of the work function of the surface. In addition to the electrostatic contribution there is also a shift in the Fermi level of the surface towards lower energies as a result of the additional electron transfer to gold. For a coverage corresponding to a monolayer of TDAE on gold the calculated reduction in work function is 2.36 eV. Thus, it is expected that if gold is used as an electron injecting contact in an electronic device such a modification of the gold surface will lead to a dramatic reduction of the energy barrier for charge injection into the electroactive material. This observation is also verified from experimental studies of TDAE on gold, even though in this case the observed change in the work function was considerably smaller, which probably is a result of partial TDAE coverage of the gold surface. Hopefully, our results will stimulate development of more elaborate methods for TDAE deposition to reach the theoretical limit of the work function shift.

## Acknowledgments

The authors would like to thank Dr Xavier Crispin for helpful discussions. Financial support from the Swedish Research Council (VR) and provision of computer facilities from the Swedish National Infrastructure for Computing (SNIC) are also gratefully acknowledged.

## References


Bagus P S, Staemmler V and Wöll C 2002 *Phys. Rev. Lett.* **89** 096104

Becke A D 1993 *J. Chem. Phys.* **98** 5648

Bock H, Borrmann H, Havlas Z, Oberhammer H, Ruppert K and Simon A 1991 *Angew. Chem. Int. Edn Engl.* **30** 1678–81

Campbell I H, Kress J D, Martin R L, Smith D L, Barashkov N N and Ferraris J P 1997 *Appl. Phys. Lett.* **71** 3528

Campbell I H, Rubin S, Zawodzinski T A, Kress J D, Martin R L, Smith D L, Barashkov N N and Ferraris J P 1996 *Phys. Rev.* B **54** R14321–4

Crispin X, Geskin V, Crispin A, Cornil J, Lazzaroni R, Salaneck W R and Brédas J L 2002 *J. Am. Chem. Soc.* **124** 8131

DeRenzi V, Rousseau R, Marchetto D, Biagi R, Scandolo S and del Pennino U 2005 *Phys. Rev. Lett.* **95** 046804

Fleurat-Lessard P and Volatron F 1998 *J. Phys. Chem.* A **102** 10151–8

Frisch M J, Trucks G W, Schlegel H B, Scuseria G E, Robb M A, Cheeseman J R, Montgomery J A Jr, Vreven T, Kudin K N, Burant J C, Millam J M, Iyengar S S, Tomasi J, Barone V, Mennucci B, Cossi M, Scalmani G, Rega N, Petersson G A, Nakatsuji H, Hada M, Ehara M, Toyota K, Fukuda R, Hasegawa J, Ishida M, Nakajima T, Honda Y, Kitao O, Nakai H, Klene M, Li X, Knox J E, Hratchian H P, Cross J B, Bakken V, Adamo C, Jaramillo J, Gomperts R, Stratmann R E, Yazyev O, Austin A J, Cammi R, Pomelli C, Ochterski J W, Ayala P Y, Morokuma K, Voth G A, Salvador P, Dannenberg J J, Zakrzewski V G, Dapprich S, Daniels A D, Strain M C, Farkas O, Malick D K, Rabuck A D, Raghavachari K, Foresman J B, Ortiz J V, Cui Q, Baboul A G, Clifford S, Cioslowski J, Stefanov B B, Liu G, Liashenko A, Piskorz P, Komaromi I, Martin R L, Fox D J, Keith T, Al-Laham M A, Peng C Y, Nanayakkara A, Challacombe M, Gill P M W, Johnson B, Chen W, Wong M W, Gonzalez C and Pople J A 2004 *n.d. 'Gaussian 03, Revision C.02'* (Wallingford, CT: Gaussian)

Hay P J and Wadt W R 1985 *J. Chem. Phys.* **82** 299

Heimel G, Romaner L, Bredas J L and Zojer E 2006 *Phys. Rev. Lett.* **96** 196806

Henkelman G, Arnaldsson A and Jónsson H 2006 *Comput. Mater. Sci.* **36** 354–60

Kresse G and Furthmüller J 1996a *Comput. Mater. Sci.* **6** 15

Kresse G and Furthmüller J 1996b *Phys. Rev.* B **54** 11169

Kresse G and Hafner J 1993 *Phys. Rev.* B **47** R558

Kristyan S and Pulay P 1994 *Chem. Phys. Lett.* **229** 175

Lang N D 1971 *Phys. Rev.* B **4** 4234

Lee C, Yang W and Parr R G 1988 *Phys. Rev.* B **37** 785

Lewis S P and Rappe A M 1999 *J. Chem. Phys.* **110** 4619–33

Lindell L, Unge M, Osikowicz W, Stafström S, Salaneck W, Crispin X and de Jong M 2008 *Appl. Phys. Lett.* **92** 163302

Lüth H 1995 *Surface and Interfaces of Solid Materials* (Berlin: Springer)

Neugebauer J and Scheffler M 1992 *Phys. Rev.* B **46** 16067–80

Osikowicz W, Crispin X, Tengstedt C, Lindell L, Kugler T and Salaneck W R 2004 *Appl. Phys. Lett.* **85** 1616

Pederson M R and Laouini N 1999 *J. Cluster Sci.* **10** 557

Perdew J P, Burke K and Ernzerhof M 1996 *Phys. Rev. Lett.* **77** 3865–8

Pokhodnia K I, Papavassilliou J, Umek P, Omerzu A and Mihailovic D 1999 *J. Chem. Phys.* **110** 3606–11

Reed A E, Weinstock R B and Weinhold F 1985 *J. Chem. Phys.* **83** 735

Rusu P C and Brocks G 2006 *Phys. Rev.* B **74** 073414

Salomon A, Berkovich D and Cahen D 2003 *Appl. Phys. Lett.* **82** 1051

Salzer Y and Cahen D 2001 *Adv. Mater.* **13** 508

Sanville E, Kenny S, Smith R and Henkelman G 2007 *J. Comput. Chem.* **28** 899–908

Sellers H, Ulman A, Shnidman Y and Eilers J E 1993 *J. Am. Chem. Soc.* **115** 9389

Silva J L F D, Stampfl C and Scheffler M 2003 *Phys. Rev. Lett.* **90** 066104

Tanaka K, Sato T and Yamabe T 1996 *J. Phys. Chem.* **100** 3980

Topping J 1927 *Proc. R. Soc.* A **114** 67–72

Vilan A, Shanzer A and Cahen D 2000 *Nature* **404** 166

Witte G, Lukas S, Bagus P S and Wöll C 2005 *Appl. Phys. Lett.* **87** 263502